J Mater Sci (2007) 42:2304–2308
DOI 10.1007/s10853-006-0180-y

Thermal-lens study of thermo-optical properties of tellurite glasses

V. Pilla · E. F. Chillcce · A. A. R. Neves · E. Munin · T. Catunda · C. L. Cesar · L. C. Barbosa

Received: 4 November 2005 / Accepted: 10 April 2006 / Published online: 23 January 2007

Abstract Mode-mismatched Thermal Lens (TL) measurements were performed in $70TeO_2$–$19WO_3$–$7Na_2O$–$4Nb_2O_5$ (% mol) tellurite glasses doped with either Er^{3+} or Tm^{3+} and co-doped with Er^{3+}/Tm^{3+} ions. Thermo-optical parameters (D, K, ds/dQ and ds/dT) were obtained in function of thulium concentrations $(0.39–1.6) \times 10^{20}$ ions/cm^3. For Er^{3+}/Tm^{3+} co-doped tellurite glasses, D and K values are practically independent of the Tm^{3+} concentrations used in this study. The average values of D and ds/dT obtained for tellurite glasses are: $(3.1 \pm 0.2) \times 10^{-3}$ cm^2/s and $(16 \pm 3) \times 10^{-6}$ K^{-1}, respectively.

Introduction

Tellurite glass has been receiving special attention because it possesses interesting properties as: high rare earth ions solubility, higher refractive indices than both the silicates and fluoride glasses, and large amplification bandwidth. In this way, tellurite glasses are becoming promising for practical applications as: optical amplifiers, optical recording, laser active media and infrared-to-visible converters [1–6]. The studies of these optical materials are driven by a strong interest do gather fundamental material properties that could lead to the development of new solid-state short-wavelength laser. For example, Er^{3+}/Eu^{3+} co-doped tellurite fibre presents visible emission [5], being a potential host material for satellite communication at 589 nm and a compact fibre laser for medical application at 613 nm. In addition, Er^{3+}/Tm^{3+} co-doped tellurite glasses present blue up-conversion, as the Er^{3+} ion plays the role of a selective sensitizer for the Tm^{3+} ion [6]. In this way, the characterizations of the nonlinear optical and thermo-optical properties of the tellurite glasses are very important for the optimization of the applications of these materials.

The characterization of the thermooptic properties is fundamental for the determination of the thermo-mechanical figure of merit of optical materials. In this form, it becomes possible to determine parameters as: thermal-shock, thermal fracture resistance and thermal lens effect [7–9]. The thermal diffusivity (D) and thermal conductivity (K) measure the rate of change of temperature in a transient heat transfer process. Usually, D and K are dependent upon processing condition and the compositional and structural properties of the glass. For instance, the improvement of a laser material performance, a high thermal conductivity is desirable to dissipate the heat from regions in which generation of laser light occurs. On the other hand, the optical path S (cm) of the glass with refractive index n and thickness L is dependent on the temperature ($S(T) = n(T)\ L(T)$) and the thermally

V. Pilla (✉) · E. Munin
Instituto de Pesquisa e Desenvolvimento- IPD, Universidade do Vale do Paraíba- Univap, São José dos Campos 12244-000, SP, Brazil
e-mail: vpilla@univap.br

E. F. Chillcce · A. A. R. Neves · C. L. Cesar · L. C. Barbosa
Instituto de Física Gleb Wataghin, Universidade Estadual de Campinas- Unicamp, Campinas 13083-970, SP, Brazil

T. Catunda
Instituto de Física de São Carlos, Universidade de São Paulo- Usp, São Carlos 13560-970, SP, Brazil

induced distortion of a laser beam during its passing through a sample is described by the optical path-length change ($ds/dT = L^{-1}\ dS/dT$). The search for athermal glasses, which minimizes temperature-related beam distortions, is very important to improve performance of optical systems as laser oscillators and telescopes in artificial satellites [7]. Then, the knowledge of thermal parameters of the materials, can be used into the development of novel materials by modifications of the composition, preparation or combinations of different optical materials [10], trying to take advantage of the merits of each material.

Thermal studies have been made in different kinds of glass host structures using Thermal Lens (TL) technique. Published data are restricted to fluoroindate, silica calcium aluminosilicate, chalcogenide and phosphate glasses single-doped with Er^{3+}, Tm^{3+}, Nd^{3+}or Yb^{3+} ions [7, 11–15]. In this work, we studied the thermooptics properties of Er^{3+}/Tm^{3+} co-doped tellurite glasses as a function of the thulium (Tm_2O_3) concentration. The TL measurements were performed by using a probe beam from a $\lambda_p = 632.8$ nm He–Ne laser. The wavelengths of $\lambda_e = 488$, 785 and 800 nm were used for excitation. For either Er^{3+} or Tm^{3+} doped and also for the Er^{3+}/Tm^{3+} co-doped tellurite glasses, the thermooptic properties such as: D, K and ds/dT were determined, as well as the thermal lens distortion induced by the pump beam (ds/dQ).

Mode-mismatched TL technique theory

The TL effect can be treated through the calculation of the temporal evolution of the sample temperature profile $\Delta T(r,t)$, caused by a Gaussian intensity distribution of the excitation beam, absorbed by the sample. The propagation of a probe beam through this thermal lens results in a variation of its on-axis intensity, $I(t)$, which can be calculated in *cw* excitation regime, in the form [7, 16]:

$$I(t) = I(0)\left[1-\frac{\theta}{2}\tan^{-1}\left(\frac{2mV}{\left[(1+2m)^2+V^2\right]\tau_c/2t+1+2m+V^2}\right)\right]^2 \quad (1)$$

where $m = (w_p/w_e)^2$, w_p and w_e are respectively the probe and excitation beam radius at the sample; $V = z_1/z_o$, z_1 is the distance between the sample and the probe beam waist and z_o is the probe beam Rayleigh range; $I(0)$ is the on-axis intensity when t, or θ, is zero. τ_c is the characteristic heat diffusion time, given by [7]:

$$\tau_c = \frac{w_e^2}{4D} \quad (2)$$

where $D = K/\rho C$ is the thermal diffusivity (cm^2/s), K is the thermal conductivity ($Js^{-1}cm^{-1}K$), ρ is the density (g/cm^3) and C is the specific heat (J/gK).

The TL transient signal amplitude, θ, is approximately the phase difference of the probe beam at $r = 0$ and $r = \sqrt{2}\ w_e$ induced by the pump beam. The normalized phase shift, $\Theta = -\theta/P_e\alpha L_{eff}$, can be expressed as [17]:

$$\Theta = \left[\frac{1}{D\lambda_p}\varphi\right]\frac{ds}{dQ} \quad (3)$$

where $P_e(W)$ is the excitation power, α (cm^{-1}) the optical absorption coefficient at the excitation wavelength (λ_e), $L_{eff} = (1-e^{-\alpha L})/\alpha$ is the effective length and L(cm) is the sample thickness. φ is the fraction of absorbed energy converted into heat or absolute nonradioative quantum efficiency [16, 18, 19].

The first term in parenthesis on the right-hand side of Eq. (3) is the energy deposited by the pumping beam within a probe beam with characteristic volume consisting of a cylinder of unit area and length equal to the probe beam wavelength, λ_p. The term ds/dQ is the sample characteristic response function describing how the optical path-length change (ds/dT) with the heat deposited per volume, in the form:

$$\frac{ds}{dQ} = \frac{1}{\rho C}\frac{ds}{dT} \quad (4)$$

For glasses, the thermal expansion may also contribute to the temperature coefficient of the optical path, according to [20, 21]:

$$\frac{ds}{dT} = \frac{dn}{dT} + \beta(n-1)(1+v) + \frac{\beta}{4}n^3 Y\left(q_\perp + q_{||}\right) \quad (5)$$

where β is the expansion coefficient, v is the Poisson's ratio, n is the refractive index, Y the Young's modulus, $q_\perp$ and $q_{||}$ are stress-optic coefficients for the parallel and perpendicular orientation relative to excitation beam polarization. The Eq. (5) takes into account the refractive index change, thermal expansion and photoelastic effect. The term dn/dT, the thermooptic coefficient, is given by [22]:

$$\frac{dn}{dT} = \frac{(n^2-1)(n^2+2)}{6n^2}\left[\frac{1}{\gamma}\frac{d\gamma}{dT} - 3\beta\right] \quad (6)$$

where 3β (K^{-1}) is the volume expansion coefficient and γ is the polarizability. As shown in Eq. (6), dn/dT is affected by two counteracting factors. First, a decrease in the density due to thermal expansion decreases the refractive index because of the larger intermolecular spacing. Second, an increase in the electronic polarizability causes the refractive index to gradually increase. In liquids, dn/dT is usually negative because the thermal expansion is the dominant term in Eq. (6). For glasses and transparent crystals, dn/dT can be either positive or negative, depending on the glass structure. For examples, the silica glasses have positive $dn/dT = +9.3 \times 10^{-6}\ K^{-1}$ values and fluoride glasses, as fluorozirconate presents negative $dn/dT = -14.5 \times 10^{-6}\ K^{-1}$ value [7, 23]. In a general form, dn/dT is negative for highly expansive and loosely bound networks and positive for strongly bound networks. Polymers usually have high expansion coefficients and dn/dT is negative, for instance, undoped PVA/GLUT-PAni film has a $dn/dT = -1.30 \times 10^{-4}\ K^{-1}$ [17].

Experimental

The tellurite glass composition used in this work was 70 mol% of TeO_2, 19 mol% of WO_3, 7 mol% of Na_2O and 4 mol% of Nb_2O_5. The raw materials (Ceraco with purity 99.99 wt%) and the rare earth ions in the form of oxides (Er_2O_3 and/or Tm_2O_3) were mixed, melted and homogenized in platinum crucible at 800°C during 30 min using a RF induction furnace. The batch size was 60 g. For the single-doped tellurite glass an amount of 7500 ppm (1.19×10^{20} ions/cm^3) of Er_2O_3 or 5000 ppm (0.78×10^{20} ions/cm^3) of Tm_2O_3 was added. For the Er^{3+}/Tm^{3+} co-doped Tellurite samples, 7500 ppm of Er_2O_3 and (2500–10,000) ppm (or 0.39–1.6×10^{20} ions/cm^3) of Tm_2O_3 were added (Table 1).

The spectral measurements of attenuation coefficient were carried out with a Perkin Elmer Lambda 9 spectrophotometer at room temperature, with resolution of 1 nm.

The thermooptic properties of Er^{3+}/Tm^{3+} co-doped tellurite glasses with different concentrations of thulium ion, were investigated by the TL method [7, 16, 17]. The TL transient measurements were performed using the mode-mismatched dual-beam (excitation and probe) configuration. A He–Ne laser ($\lambda_p = 632.8$ nm) was used as the probe beam and either an Ar^+ laser ($\lambda_e = 488$ nm) or a Ti-sapphire laser ($\lambda_e = 785$ or 800 nm) was used to provide the excitation beam. Details of the experimental setup is described elsewhere [7, 16]. The optical absorption coefficients (α) were determined considering the reflections at the sample surface and applying the same experimental configuration of the TL measurements.

Results and discussions

The preparation procedure produced bubble-free transparent glasses with high homogeneity, as observed by Shadowgraphy technique. The compositions of the glasses obtained were analyzed by X-ray fluorescence spectroscopy (EDX-700). Although it is a semi quantitative technique, the composition change due to vaporization was limited to less than 6% for all components of all samples.

Attenuation coefficient spectra of Er^{3+} doped, Tm^{3+} doped and Er^{3+}/Tm^{3+} co-doped tellurite glasses are presented in the Fig. 1(a–c), respectively. The refractive index of these glasses as a function of the

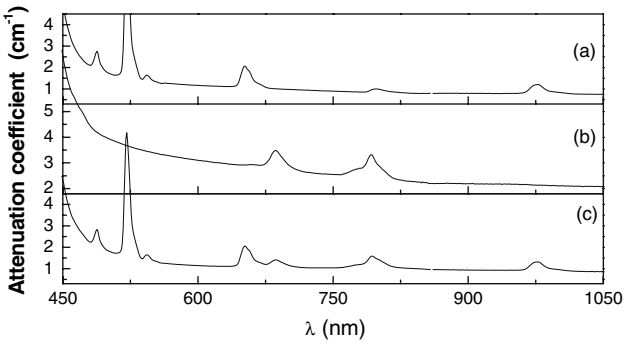

Fig. 1 Attenuation coefficient ($-\ln(I/I_0)/L$) of tellurite glasses: (**a**) $S_{7.5,0}$; (**b**) $S_{0,5.0}$ and (**c**) $S_{7.5,2.5}$

Table 1 Thermal properties of tellurite glasses

Tellurite	Er^{3+} (ppm)	Tm^{3+} (ppm)	ρ (± 0.1 g /cm^3)	D (10^{-3} cm^2/s)	K (10^{-3} W/ K cm)	ds/dQ (10^{-6} cm^3/J)	ds/dT (10^{-6} K^{-1})
$S_{0,0}$	0	0	5.7	3.0 ± 0.2	8	4.4	11.7
$S_{0,5}$	0	5000	5.6	3.2 ± 0.4	8.4	6.23	16.4
$S_{7.5,0}$	7500	0	5.5	3.1 ± 0.2	8	6.73	17.4
$S_{7.5,2.5}$	7500	2500	5.6	3.0 ± 0.2	7.9	7.52	19.8
$S_{7.5,5}$	7500	5000	5.6	3.0 ± 0.3	7.9	5.32	14
$S_{7.5,7.5}$	7500	7500	5.5	3.3 ± 0.1	8.5	5.42	14
$S_{7.5,10}$	7500	10,000	5.6	3.1 ± 0.3	8.2	4.83	12.7

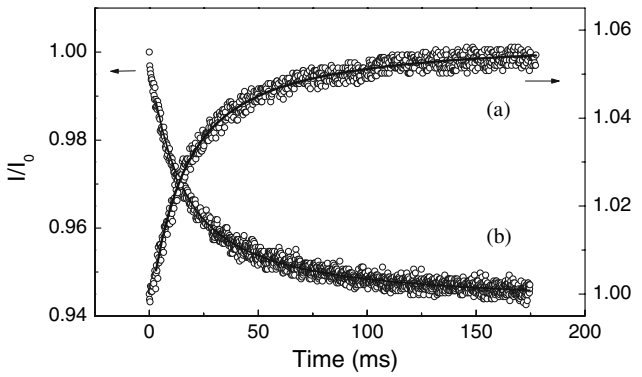

Fig. 2 TL transient signal for (**a**) tellurite undoped glass and (**b**) ZBLAN (0.58% CoF_2). The sample was excited with an Ar^+ laser at 488 nm with $P_e \approx 9.2$ mW and probe laser beam at $\lambda_p = 632.8$ nm. The line curve is the fit curve obtained by Eq. (1)

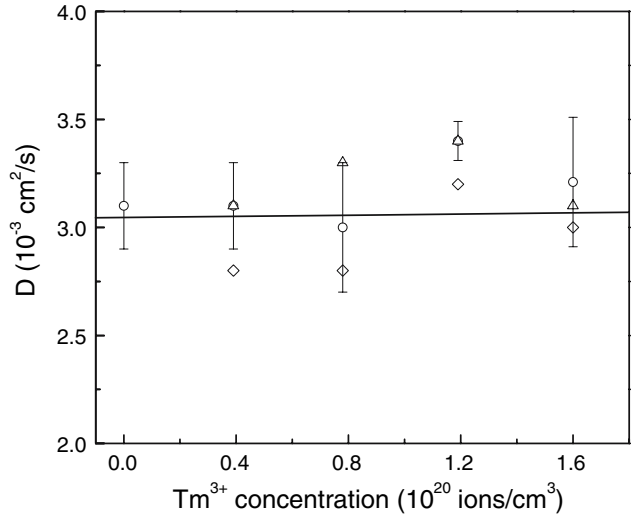

Fig. 3 D in function of Thulium concentration for samples of Er^{3+}/Tm^{3+} co-doped tellurite glasses at 488 nm (open circle), 785 nm (open diamond) and 800 nm (open triangle)

wavelength (λ in nm) can be expressed as: $n(\lambda) \approx (1 + 3.24\lambda^2/(\lambda^2–193^2))^{0.5}$ [4]. Fresnel reflection coefficients, described by the equation ($R = [(n(\lambda)–1)/(n(\lambda)+1)]^2$), can be used to understand the rising of the baseline at short wavelengths in Fig. 1(a–c).

Figure 2 shows a typical TL transient signal for (a) an undoped tellurite and (b) fluorozirconate ZBLAN (0.56% CoF_2) glass. Fitting the experimental data of

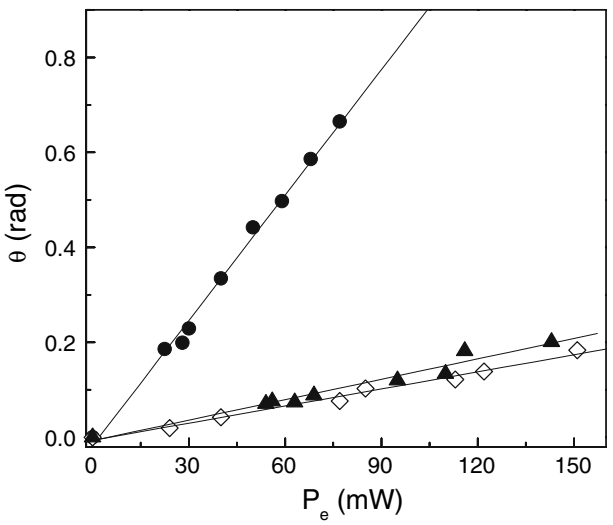

Fig. 4 θ in function of P_e for tellurite glass $S_{7.5,2.5}$ at 488 nm (closed circle), 785 nm (open diamond) and 800 nm (open triangle)

Fig. 2 by Eq. (1), the following values for the equation parameters were obtained (a) $\theta = –(0.0597 \pm 0.0004)$ rad and $\tau_c = (0.573 \pm 0.008)$ ms and (b) $\theta = (0.0542 \pm 0.0002)$ rad and $\tau_c = (0.621 \pm 0.005)$ ms, for tellurite and ZBLAN, respectively. From Eq. (2) and using the measured value $w_e = 2.6 \times 10^{-3}$ cm, the thermal diffusivity $D = (2.9 \pm 0.2) \times 10^{-3}$ cm^2/s was determined for undoped tellurite glass. The same procedure above to determine D was developed on the ZBLAN ($D = (2.8 \pm 0.2) \times 10^{-3}$ cm^2/s), Er^{3+} doped, Tm^{3+} doped and Er^{3+}/Tm^{3+} co-doped tellurite glasses. In the Fig. 3 are presented D values obtained for Er^{3+}/Tm^{3+} co-doped tellurite samples in function of the concentration of thulium ion for three different excitation wavelengths (λ_e = 488, 785 or 800 nm). The average value of $D = (3.1 \pm 0.1) \times 10^{-3}$ cm^2/s obtained for tellurite doped samples (Er^{3+}, Tm^{3+} and Er^{3+}/Tm^{3+}) is similar to the values obtained in the literature for the glasses showed in the Table 2 and others several fluoride glasses as: YABC, PGIZCa, ISZn and InS-BZnGdN [7, 14]. In the Fig. 3, no significant change can be observed for the thermal diffusivity D for the thulium concentration range studied in this work, as the small differences in D values are within the error bars.

Table 2 Thermal properties of glasses

Glasses	D (10^{-3} cm^2/s)	K (10^{-3} W/Kcm)	ds/dT (10^{-6} K^{-1})	ds/dQ (10^{-6} cm^3/J)
ZBLAN (0.38 CoF_2) [11]	(2.7 ± 0.1)	(8.0 ± 0.7)	–(6.4 ± 0.9)	–(2.1 ± 0.9)
Soda lime [10]	(4.9 ± 0.2)	(10 ± 1)	(2.1 ± 0.2)	(1.3 ± 0.1)
Tellurite	(3.1 ± 0.2)	(8.0 ± 0.2)	(16 ± 3)	(6 ± 1)
LSCAS [22]	(5.7 ± 0.3)	(16 ± 2)	(6.2 ± 0.6)	(2.3 ± 0.2)
GaLaS [10]	(2.7 ± 0.1)	(4.3 ± 0.4)	(2.6 ± 0.3)	(1.6 ± 0.2)

The curve behavior of Fig. 2(a) indicates that d*s*/d*Q* (proportional to d*s*/d*T)* is positive for tellurite matrix, i.e., the created TL focalize the probe beam in the far field. For the sake of comparison, Table 2 lists positive d*s*/d*T* values for chalcohalide, chalcogenide, soda lime, LSCAS and GaLaS. For ZBLAN, $ds/dT = -(7.8 \pm 0.9) \times 10^{-6}\,K^{-1}$ is negative and the beam is defocused in the far field. A typical transient curve for that case is shown in Fig. 2(b). Fluoride, fluroaluminate and fluorindate glasses are also characterized by negative value of d*s*/d*T* [11, 15, 21]. d*s*/d*Q values* can be obtained from θ by using Eq. (1) and the values of D, λ_p and φ in the Eq. (3). For tellurite glasses studied in this work, we considered $\varphi = 1$ and the average value obtained was $ds/dQ = (6 \pm 1) \times 10^{-6}\,cm^3/J$. In Fig. 4, the values of θ are presented in function of P_e employing using as pump-beam in the TL technique either an Ar^+ laser (λ_e = 488 nm) or a Ti-sapphire laser (λ_e = 785 or 800 nm) for Er^{3+}/Tm^{3+} co-doped tellurite glass ($S_{7.5,2.5}$). A linear behavior is observed in the used power range.

In order to obtain K and d*s*/d*T*, ρ and C must be known. We assumed that C for Er^{3+}/Tm^{3+} co-doped tellurite glass is the same of the undoped tellurite glass. Therefore, using the value of D, ρ, d*s*/d*Q* (Table 1) and $C = 0.47$ J/gK [24] we obtained the following average values: $K = (8.1 \pm 0.2) \times 10^{-3}$ W/cmK and $ds/dT = (16 \pm 3) \times 10^{-6}\,K^{-1}$. For tellurite glass the value of d*s*/d*T* is approximately two times larger than that obtained for low silica calcium aluminosilicate LSCAS (Table 2). Negleting the photoelastic effect in the Eq. (5), with $\beta = (14 \pm 3) \times 10^{-6}/°C$, $\nu = (0.33 \pm 0.03)$ and $n = 2.14$ [4, 25, 26] it is possible calculate average value of $dn/dT = -8 \times 10^{-6}\,K^{-1}$ for tellurite glasses. For comparation, ZBLAN glass has a $dn/dT = -14 \times 10^{-6}\,K^{-1}$ and fluorozirco-aluminate glass $dn/dT = -6 \times 10^{-6}\,K^{-1}$ [11]. Modifications in the glass matrix aiming an increase in $|dn/dT|$ are required for obtaining an athermal tellurite glass.

Conclusions

In conclusion, we have applied the Thermal Lens (TL) technique to characterize tellurite ($70\%TeO_2$–$19\%WO_3$–$7\%Na_2O$–$4\%Nb_2O_5$) doped and co-doped with rare earth (E_2O_3 and Tm_2O_3) glasses at different excitation wavelength (488, 785 and 800 nm). For Er^{3+}/Tm^{3+} co-doped tellurite samples the measurements of TL were performed in function of thulium concentration. d*s*/d*T* presented average variations of 27% with the insertion of thulium and erbium in tellurite matrix. No significant changes were observed for the values of D for different doping levels.

Acknowledgement This research was supported by FAPESP, PRONEX and CEPOF.

References

1. Tanabe S, Hirao K, Soga N (1990) J Non-Cryst Solids 122:79
2. Ryba-Romanowski W (1990) J Lumin 46:163
3. Inoue S, Nukui A, Yamamoto K, Yano T, Shibata S, Yamane M (2002) J Mater Sci 37:3459
4. Chillcce EF, Rodriguez E, Neves AAR, Moreira WC, César CL, Barbosa LC (2006) Opt Fiber Tech 12:185
5. Huang L, Jha A, Shen S, Chung WJ (2004) Opt Commun 239:403
6. Tanabe S, Suzuki K, Soga N, Hanada T (1995) J Lumin 65:247
7. Lima SM, Sampaio JA, Catunda T, Bento AC, Miranda LCM, Baesso ML (2000) J Non-Cryst Solids 273:215
8. Woods BW, Payne SA, Marion JE, Hughes RS, Dovis LE (1991) J Opt Soc Am B 8:970
9. Payne SA, Smith LK, Beach RJ, Chai BHT, Tassano JH, Deloach LD, Kway WL, Solarz RW, Krupke WF (1994) Appl Opt 33:5526
10. Pilla V, Andrade AA, Lima SM, Catunda T, Donatti DA, Vollet DR, Ruiz AI (2003) Opt Mat 24:483
11. Lima SM, Sampaio JA, Catunda T, Lebullenger R, Hernandes AC, Baesso ML, Bento AC, Gandra FCG (1999) J Non-Cryst Solids 256&257:337
12. Baesso ML, Bento AC, Duarte AR, Neto AM, Miranda LCM, Sampaio JA, Catunda T, Gama S, Gandra FCG (1999) J Appl Phys 85:8112
13. Sampaio JA, Catunda T, Gandra FCG, Gama S, Bento AC, Miranda LCM, Baesso ML (1999) J Non-Cryst Solids 247:196
14. Lima SM, Catunda T, Lebullenger R, Hernandes AC, Baesso ML, Bento AC, Miranda LCM (1999) Phys Rev B 60:15173
15. Lima SM, Sampaio JA, Catunda T, Camargo ASS, Nunes LAO, Baesso ML, Hewak DW (2001) J Non-Cryst Solids 284:274
16. Pilla V, Lima SM, Catunda T, Medina A, Baesso ML, Jenssen HP, Cassanho A (2004) J Opt Soc Am B 21:1784
17. Pilla V, Catunda T, Balogh DT, Faria RM, Zilio SC (2002) J Polym Sc, Part B Polym Physics 40:1949
18. Pilla V, Catunda T, Jenssen HP, Cassanho A (2003) Opt Lett 28:239
19. Andrade AA, Lima SM, Pilla V, Sampaio JA, Catunda T (2003) Rev Sci Instrum 74:857
20. Shen J, Baesso ML, Snook RD (1994) J Appl Phys 75:3738
21. Lima SM, Andrade AA, Catunda T, Lebullenger R, Smektala F, Jestin Y, Baesso ML (2001) J Non-Cryst Solids 284:203
22. Rohling JH, Caldeira AMF, Pereira JRD, Medina AN, Bento AC, Baesso ML, Miranda LCM, Rubira AF (2001) J Appl Phys 80:2220
23. Jewell JM, Apkins C, Aggarwal ID (1991) Appl Opt 30:3656
24. Lima SM, Falco WF, Bannwart ES, Andrade LHC, Oliveira RC, Moraes JCS, Yukimitu K, Araújo EB, Falcão EA, Steimacher A, Astrath NGC, Bento AC, Medina AN, Baesso ML (2006) J Non-Cryst Solids 352:3603
25. Sidlkey MA, El-Mallawany R, Nakhla RI, Abdelmoneim A (1997) J Non-Cryst Solids 215:75
26. El-Mallawany RAH (2001) Tellurite Glasses Handbook: Physical Properties and Data, CRC PRESS Page. 205